State Estimation Based Fault Location Method for Active Distribution Networks

Binglin Wang[1], *Student Member, IEEE*, Yu Liu[1,2,*], *Member, IEEE*, Junbo Zhao[3], *Member, IEEE*, Yixiong Jia[1], *Student Member, IEEE*, and Xinyu Chen[4]
1. School of Information Science and Technology, ShanghaiTech University, Shanghai, China, 201210
2. Key Laboratory of Control of Power Transmission and Conversion (SJTU), Ministry of Education, Shanghai, 200240
3. Department of Electrical and Computer Engineering, Mississippi State University, Starkville, MS, 39762, USA
4. State Grid Huaian Electric Power Supply Company, Huaian, Jiangsu, 223002, China,
*Email: liuyu.shanghaitech@gmail.com

Abstract: This paper proposes a novel fault location method for active distribution networks. The voltage and current phasor measurements at each terminal of the network are typically required. The overall model of the active distribution network with fault is established with the distribution line model of each section. The three phase matrix representation of physical laws of the distribution line is utilized to consider the asymmetrical distribution circuit. Moreover, the line shunt admittance can be considered in the proposed method to obtain more accurate fault location results. The proposed fault location algorithm first identifies the faulted line section and afterwards adopts state estimation method to identify the fault location. The benefits of considering line shunt admittances are also discussed. Numerical experiments verify that the proposed method can work for the unbalanced distribution system and asymmetrical lines. It is also shown that the consideration of line shunt admittances yields better fault location results.

Key words: Active distribution network, systematic network model, line shunt admittance, unbalanced system, state estimation

I. INTRODUCTION

ACCURATE fault location is of vital significance for safety, reliable and high power quality of the distribution system. Active distribution networks with distributed generations (DGs) enable a high penetration of renewables as well as optimized operation and control of distribution systems. Nevertheless, the fault location in active distribution networks could be challenging due to bi-directional power flow and complex fault characteristics. Owing to the specific topological and operational characteristics, fault location in distribution network is often performed through visual inspection and field investigation [1]. These methods are not feasible for underground systems and usually require long time to obtain accurate location results. Existing fault location methods in distribution system mainly include impedance based and traveling wave based methods. Moreover, the power quality monitoring data based and artificial intelligence based methods are also applied in the distribution system [2].

Specifically，impedance based fault location methods utilize the proportional relationship between the fault location and the line impedance (between one terminal of the circuit and the fault). An impedance based single ended method considering load characteristic is proposed in [3]. The fault location is estimated by equating the imaginary part of the fault impedance to zero. However, the shunt capacitance of the distribution line is not considered. This issue is addressed in [4]. The fault location is obtained by solving the fault location equation. However, they treat the lines as geometrically symmetrical by using sequence domain networks. This assumption may generate fault location errors. Moreover, researchers also proposed direct circuit analysis based fault location methods in [5-6]. The matrix inverse lemma is utilized and a quadratic polynomial with respect to the fault location is derived. Although this method can work for the unbalanced distribution system, there will be multiple candidate locations and the identification among these locations is still challenging. In addition, the method does not consider line to ground capacitive currents, which may generate fault location errors.

For the traveling wave based fault location method, the time difference of the arrival time of traveling wave fronts is utilized to determine the fault location. For single ended traveling wave based fault location methods [7], the fault location is determined via the arrival time of the traveling wave reflections at the local end of the line and the propagation velocity. For multi ended traveling wave based fault location methods [8], the fault location is determined via the first arrival time of the traveling waves generated by the fault. Traveling wave based fault location methods in distribution networks could still be challenging due to the following reasons. First, the traveling wave propagation could be extreme complicated due to the existence of large number of branches in the distribution system, and the calculated electrical distance at the measurement units may correspond to several fault locations [9]. Second, the accuracy of this method is dependent on the reliable detection of wavefronts, which might be problematic during faults with high impedances or zero inception angles. Third, measurement devices with high sampling rates are typically required.

To ensure the reliable and stable operation of the distribution system, distribution automation has been widely applied in distribution system, including real-time monitoring, coordination and operation equipment. Therefore, the fault location methods based on the power quality monitoring data have been investigated. In [10], the fault indicator is utilized for the fault location algorithm. In [11], the power line communication devices are leveraged to achieve location of the high impedance faults. In [12], the voltage sag characteristic is used for the fault location via installed power quality meters. These methods are usually dependent on the installation of additional measurement devices with specific functions.

This work is sponsored by National Nature Science Foundation of China (No. 51807119), Shanghai Pujiang Program (No. 18PJ1408100) and Key Laboratory of Control of Power Transmission and Conversion (SJTU), Ministry of Education (No. 2015AB04). Their support is greatly appreciated.

978-1-7281-5508-1/20/$31.00 ©2020 IEEEI978-1-7281-5508-1/20/$31.00 ©2020 IEEEE978-1-7281-5508-1/20/$31.00 ©2020 IEEEE978-

Moreover, the reliable data at all devices should be appropriately managed for the accurate fault location results.

Artificial intelligence based fault location methods are emerging in distribution networks. The intelligent fault diagnosis algorithm is applied to identify the fault location among multiple candidate locations using current pattern information of the protective device and interrupted load information [13]. In [14], the learning algorithm for multivariable data analysis is utilized to locate faults. The massive voltage and current waveforms during the fault events are trained to obtain a set of descriptors. However, the artificial intelligence based methods require a large amount of high-quality data which is difficult to acquire.

In this paper, a novel fault location method for active distribution networks is proposed. Three phase voltage and current phasor measurements at each terminal of the network are assumed. The method first establishes an overall model of the active distribution network with fault, where the location of the fault is introduced as a state of the system. Afterwards, state estimation approach is adopted to identify the fault location. This method can systematically consider the network configuration, the shunt admittance, and the asymmetry of the distribution line. The effectiveness of the method is not affected by system imbalance, varying loads, and different operating conditions of DGs. The rest of the paper is arranged as follows. Section II introduces the systematic modeling procedure of the distribution network. Section III proposes the state estimation based fault location algorithm. Section IV demonstrates the numerical simulation results of the proposed method. Section V draws the conclusion.

II. Modeling of Distribution Network

The overall distribution network model is composed of the line model of each section. In this section, the line model of each section with and without considering the shunt admittance is firstly developed. Afterwards, the systematic modeling procedure of the overall network is derived.

A. Line model of each section

Assume the terminal three phase voltage measurements at S end and R end are $\tilde{\boldsymbol{U}}_S$ and $\tilde{\boldsymbol{U}}_R$ respectively, and the terminal three phase current measurements flowing into S end and R end are $\tilde{\boldsymbol{I}}_S$ and $\tilde{\boldsymbol{I}}_R$ respectively. The impedance and admittance matrices of the per unit length line are $\boldsymbol{Z}$ and $\boldsymbol{Y}$. The length of the line section is d and the distance from the fault to the S end is d_1. The equivalent circuits of a distribution line section (normal operating condition or fault condition; with or without shunt admittance) are shown in Figure 1. Note that the following models adopt three phase matrix representation of physical laws instead of sequence networks, and therefore can be utilized in asymmetrical distribution circuits.

(1) Normal operating condition model without admittance

From Figure 1(a), the line section can be represented as,

$$\begin{aligned}
\tilde{\boldsymbol{U}}_R^{(\mathrm{Re})} &= \tilde{\boldsymbol{U}}_S^{(\mathrm{Re})} - d\cdot\left(\boldsymbol{Z}^{(\mathrm{Re})}\tilde{\boldsymbol{I}}_L^{(\mathrm{Re})} - \boldsymbol{Z}^{(\mathrm{Im})}\tilde{\boldsymbol{I}}_L^{(\mathrm{Im})}\right)\\
\tilde{\boldsymbol{U}}_R^{(\mathrm{Im})} &= \tilde{\boldsymbol{U}}_S^{(\mathrm{Im})} - d\cdot\left(\boldsymbol{Z}^{(\mathrm{Im})}\tilde{\boldsymbol{I}}_L^{(\mathrm{Re})} + \boldsymbol{Z}^{(\mathrm{Re})}\tilde{\boldsymbol{I}}_L^{(\mathrm{Im})}\right)\\
\tilde{\boldsymbol{I}}_S^{(\mathrm{Re})} &= \tilde{\boldsymbol{I}}_L^{(\mathrm{Re})},\ \tilde{\boldsymbol{I}}_S^{(\mathrm{Im})} = \tilde{\boldsymbol{I}}_L^{(\mathrm{Im})}
\end{aligned} \tag{1}$$

where $\tilde{\boldsymbol{I}}_L$ is the three phase current flowing through the line from S end to R end. Superscript (Re) represents real part and (Im) represents imaginary part of the variable.

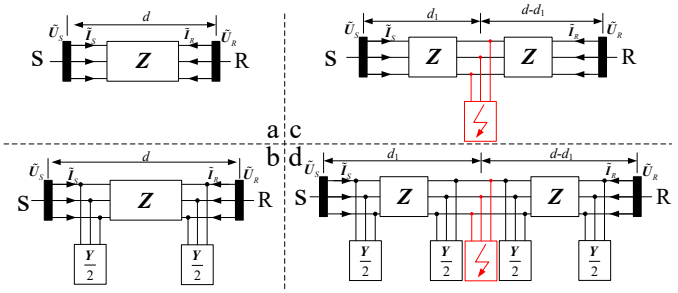

Figure 1. Equivalent circuit of a line section: (a) normal operating condition without admittance; (b) normal operating condition with admittance; (c) fault condition without admittance; (d) fault condition with admittance

(2) Normal operating condition model with admittance

From Figure 1(b), the line can be represented as,

$$\begin{aligned}
\tilde{\boldsymbol{U}}_R^{(\mathrm{Re})} &= \tilde{\boldsymbol{U}}_s^{(\mathrm{Re})} - d\cdot\left(\boldsymbol{Z}^{(\mathrm{Re})}\tilde{\boldsymbol{I}}_L^{(\mathrm{Re})} - \boldsymbol{Z}^{(\mathrm{Im})}\tilde{\boldsymbol{I}}_L^{(\mathrm{Im})}\right)\\
\tilde{\boldsymbol{U}}_R^{(\mathrm{Im})} &= \tilde{\boldsymbol{U}}_s^{(\mathrm{Im})} - d\cdot\left(\boldsymbol{Z}^{(\mathrm{Im})}\tilde{\boldsymbol{I}}_L^{(\mathrm{Re})} + \boldsymbol{Z}^{(\mathrm{Re})}\tilde{\boldsymbol{I}}_L^{(\mathrm{Im})}\right)\\
\tilde{\boldsymbol{I}}_S^{(\mathrm{Re})} &= \tilde{\boldsymbol{I}}_L^{(\mathrm{Re})} + d/2\cdot\left(\boldsymbol{Y}^{(\mathrm{Re})}\tilde{\boldsymbol{U}}_S^{(\mathrm{Re})} - \boldsymbol{Y}^{(\mathrm{Im})}\tilde{\boldsymbol{U}}_S^{(\mathrm{Im})}\right)\\
\boldsymbol{I}_S^{(\mathrm{Im})} &= \tilde{\boldsymbol{I}}_L^{(\mathrm{Im})} + d/2\cdot\left(\boldsymbol{Y}^{(\mathrm{Im})}\tilde{\boldsymbol{U}}_S^{(\mathrm{Re})} + \boldsymbol{Y}^{(\mathrm{Re})}\tilde{\boldsymbol{U}}_S^{(\mathrm{Im})}\right)
\end{aligned} \tag{2}$$

where the definitions are the same as the model in (1).

(3) Fault condition model without admittance

From Figure 1(c), the line can be represented as,

$$\begin{aligned}
\tilde{\boldsymbol{U}}_S^{(\mathrm{Re})} &= d_1\cdot\left(\boldsymbol{Z}^{(\mathrm{Re})}\tilde{\boldsymbol{I}}_{Ls}^{(\mathrm{Re})} - \boldsymbol{Z}^{(\mathrm{Im})}\tilde{\boldsymbol{I}}_{Ls}^{(\mathrm{Im})}\right) + \tilde{\boldsymbol{U}}_f^{(\mathrm{Re})}\\
\tilde{\boldsymbol{U}}_S^{(\mathrm{Im})} &= d_1\cdot\left(\boldsymbol{Z}^{(\mathrm{Im})}\tilde{\boldsymbol{I}}_{Ls}^{(\mathrm{Re})} + \boldsymbol{Z}^{(\mathrm{Re})}\tilde{\boldsymbol{I}}_{Ls}^{(\mathrm{Im})}\right) + \tilde{\boldsymbol{U}}_f^{(\mathrm{Im})}\\
\tilde{\boldsymbol{U}}_R^{(\mathrm{Re})} &= \left(d-d_1\right)\cdot\left(\boldsymbol{Z}^{(\mathrm{Re})}\tilde{\boldsymbol{I}}_{Lr}^{(\mathrm{Re})} - \boldsymbol{Z}^{(\mathrm{Im})}\tilde{\boldsymbol{I}}_{Lr}^{(\mathrm{Im})}\right) + \tilde{\boldsymbol{U}}_f^{(\mathrm{Re})}\\
\tilde{\boldsymbol{U}}_R^{(\mathrm{Im})} &= \left(d-d_1\right)\cdot\left(\boldsymbol{Z}^{(\mathrm{Im})}\tilde{\boldsymbol{I}}_{Lr}^{(\mathrm{Re})} + \boldsymbol{Z}^{(\mathrm{Re})}\tilde{\boldsymbol{I}}_{Lr}^{(\mathrm{Im})}\right) + \tilde{\boldsymbol{U}}_f^{(\mathrm{Im})}\\
\tilde{\boldsymbol{I}}_S^{(\mathrm{Re})} &= \tilde{\boldsymbol{I}}_{Ls}^{(\mathrm{Re})},\ \tilde{\boldsymbol{I}}_S^{(\mathrm{Im})} = \tilde{\boldsymbol{I}}_{Ls}^{(\mathrm{Im})},\ \tilde{\boldsymbol{I}}_R^{(\mathrm{Re})} = \tilde{\boldsymbol{I}}_{Lr}^{(\mathrm{Re})},\ \tilde{\boldsymbol{I}}_R^{(\mathrm{Im})} = \tilde{\boldsymbol{I}}_{Lr}^{(\mathrm{Im})}
\end{aligned} \tag{3}$$

where $\tilde{\boldsymbol{I}}_{Ls}$ is the three phase current flowing through S end to fault location, and $\tilde{\boldsymbol{I}}_{Lr}$ is the three phase current flowing through R end to fault location. $\tilde{\boldsymbol{U}}_f$ is the voltage at the fault location.

(4) Fault condition model with admittance

From Figure 1(d), the line can be represented as,

$$\begin{aligned}
\tilde{\boldsymbol{U}}_S^{(\mathrm{Re})} &= d_1\cdot\left(\boldsymbol{Z}^{(\mathrm{Re})}\tilde{\boldsymbol{I}}_{Ls}^{(\mathrm{Re})} - \boldsymbol{Z}^{(\mathrm{Im})}\tilde{\boldsymbol{I}}_{Ls}^{(\mathrm{Im})}\right) + \tilde{\boldsymbol{U}}_f^{(\mathrm{Re})}\\
\tilde{\boldsymbol{U}}_S^{(\mathrm{Im})} &= d_1\cdot\left(\boldsymbol{Z}^{(\mathrm{Im})}\tilde{\boldsymbol{I}}_{Ls}^{(\mathrm{Re})} + \boldsymbol{Z}^{(\mathrm{Re})}\tilde{\boldsymbol{I}}_{Ls}^{(\mathrm{Im})}\right) + \tilde{\boldsymbol{U}}_f^{(\mathrm{Im})}\\
\tilde{\boldsymbol{U}}_R^{(\mathrm{Re})} &= \left(d-d_1\right)\cdot\left(\boldsymbol{Z}^{(\mathrm{Re})}\tilde{\boldsymbol{I}}_{Lr}^{(\mathrm{Re})} - \boldsymbol{Z}^{(\mathrm{Im})}\tilde{\boldsymbol{I}}_{Lr}^{(\mathrm{Im})}\right) + \tilde{\boldsymbol{U}}_f^{(\mathrm{Re})}\\
\tilde{\boldsymbol{U}}_R^{(\mathrm{Im})} &= \left(d-d_1\right)\cdot\left(\boldsymbol{Z}^{(\mathrm{Im})}\tilde{\boldsymbol{I}}_{Lr}^{(\mathrm{Re})} + \boldsymbol{Z}^{(\mathrm{Re})}\tilde{\boldsymbol{I}}_{Lr}^{(\mathrm{Im})}\right) + \tilde{\boldsymbol{U}}_f^{(\mathrm{Im})}\\
\tilde{\boldsymbol{I}}_S^{(\mathrm{Re})} &= \tilde{\boldsymbol{I}}_{Ls}^{(\mathrm{Re})} + d_1/2\cdot\left(\boldsymbol{Y}^{(\mathrm{Re})}\tilde{\boldsymbol{U}}_S^{(\mathrm{Re})} - \boldsymbol{Y}^{(\mathrm{Im})}\tilde{\boldsymbol{U}}_S^{(\mathrm{Im})}\right)\\
\tilde{\boldsymbol{I}}_S^{(\mathrm{Im})} &= \tilde{\boldsymbol{I}}_{Ls}^{(\mathrm{Im})} + d_1/2\cdot\left(\boldsymbol{Y}^{(\mathrm{Im})}\tilde{\boldsymbol{U}}_S^{(\mathrm{Re})} + \boldsymbol{Y}^{(\mathrm{Re})}\tilde{\boldsymbol{U}}_S^{(\mathrm{Im})}\right)\\
\tilde{\boldsymbol{I}}_R^{(\mathrm{Re})} &= \tilde{\boldsymbol{I}}_{Lr}^{(\mathrm{Re})} + \left(d-d_1\right)/2\cdot\left(\boldsymbol{Y}^{(\mathrm{Re})}\tilde{\boldsymbol{U}}_R^{(\mathrm{Re})} - \boldsymbol{Y}^{(\mathrm{Im})}\tilde{\boldsymbol{U}}_R^{(\mathrm{Im})}\right)\\
\tilde{\boldsymbol{I}}_R^{(\mathrm{Im})} &= \tilde{\boldsymbol{I}}_{Lr}^{(\mathrm{Im})} + \left(d-d_1\right)/2\cdot\left(\boldsymbol{Y}^{(\mathrm{Im})}\tilde{\boldsymbol{U}}_R^{(\mathrm{Re})} + \boldsymbol{Y}^{(\mathrm{Re})}\tilde{\boldsymbol{U}}_R^{(\mathrm{Im})}\right)
\end{aligned} \tag{4}$$

where the definitions are the same as the model in (3).

B. Systematic Modeling procedure for the overall network

According to equations (1-4), the model of the network can be generated using following systematic methodology:

Step 1: *Write the model of each line section.*
Step 2: *Add the Kirchhoff's Current Law (KCL) at nodes connecting different sections.*
Step 3: *Consider the same voltages at nodes connecting different sections.*

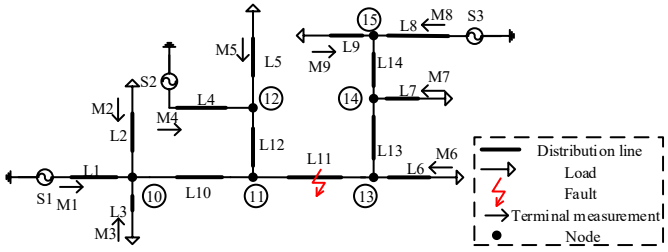

Figure 2. An example active distribution network

Next, the overall model of an example distribution network shown in Figure 2. It describes all the physical laws that the network should obey and is represented as the following general form,

$$z = f(x) \tag{5}$$

where $z = \left[z_{\text{actual}} \;\; \mathbf{0} \;\; u_{\text{actual}} \right]^T$

$$z_{\text{actual}} = \left[\tilde{U}_1^{(\text{Re})} \;\; \tilde{U}_1^{(\text{Im})} \;\; \tilde{I}_1^{(\text{Re})} \;\; \tilde{I}_1^{(\text{Im})} \;\; \cdots \;\; \tilde{U}_9^{(\text{Re})} \;\; \tilde{U}_9^{(\text{Im})} \;\; \tilde{I}_9^{(\text{Re})} \;\; \tilde{I}_9^{(\text{Im})} \right]^T$$

$$u_{\text{actual}} = \left[\tilde{U}_1^{(\text{Re})} \;\; \tilde{U}_1^{(\text{Im})} \;\; \cdots \;\; \tilde{U}_9^{(\text{Re})} \;\; \tilde{U}_9^{(\text{Im})} \right]^T$$

$$x = \left[\tilde{U}_1^{(\text{Re})} \;\; \tilde{U}_1^{(\text{Im})} \;\; \cdots \;\; \tilde{U}_{15}^{(\text{Re})} \;\; \tilde{U}_{15}^{(\text{Im})} \;\; \tilde{I}_{L1}^{(\text{Re})} \;\; \tilde{I}_{L1}^{(\text{Im})} \;\; \cdots \;\; \tilde{I}_{L9}^{(\text{Re})} \;\; \tilde{I}_{L9}^{(\text{Im})} \right.$$
$$\left. \tilde{I}_{L10-L11}^{(\text{Re})} \;\; \tilde{I}_{L10-L11}^{(\text{Im})} \;\; \cdots \;\; \tilde{I}_{L15-L14}^{(\text{Re})} \;\; \tilde{I}_{L15-L14}^{(\text{Im})} \;\; \tilde{U}_f^{(\text{Re})} \;\; \tilde{U}_f^{(\text{Im})} \;\; d_1 \right]^T$$

Function f is a set of algebraic equations, which contains the model of each section, KCLs at nodes connection different sections and actual measured state value. Detailed physical meaning of the function f is shown in Table 1.

Table 1 Physical meaning of the network model

Row index	Physical meaning
1 to 108	Normal operation line model of Line L1 to L9
109 to 156	Normal operation line model of Line L10 and L12 to L14
157 to 180	Line with fault model of Line L11
181 to 198	KCLs at node 10 to node 15
199 to 252	Actual measured state value

z is the measurement vector, including actual measurements z_{actual}, virtual zero measurements $\mathbf{0}$ and actual measured state values. Actual measurements include real and imaginary parts of voltage measurements at end M1~M9 and current measurements flowing into end M1~M9. Virtual zero measurements represent the quantities from the physical laws of the line without terminal measurements, such as KVLs of the line L11 or KCLs at the node 11. Actual state values include the real part and imaginary part of the terminal voltages. The state vector includes: real and imaginary parts of voltages at ends M1~M9 and nodes 10~15, real and imaginary parts of currents flowing into the terminals through L1~L9, real and imaginary parts of currents flowing from node 10 to 11, 11 to 13, 12 to 11, 13 to 11, 14 to 13, 15 to 14; real and imaginary parts of voltages at the fault location, and the distance between node 11 and the fault location.

Note that the overall line model of each section in equation (5) can be classified into two types: the overall model without shunt admittance and the overall model with shunt admittance. The overall model without shunt admittance utilizes equations (1) and (3) for the model of each section. By contrast, the overall model with shunt admittance utilizes equations (2) and (4) for the model of each section.

III. State Estimation Based Fault Location Method

The proposed fault location method contains two steps. The first step is to identify the line section with fault. The second step is to find the exact location of the fault.

A. Faulted line identification

The main idea of faulted line identification is to check whether the line obeys the physical laws of the line model during normal operating conditions. Here we assume that the network is only with one fault. Specifically, the faulted line identification procedure contains the following steps:

Step (a) Initialization of normal nodes

Set all terminal nodes (eg. terminal M1 to M9) to be "normal nodes". The meaning of normal nodes is that the given (or calculated) voltages at this node and currents flowing out of this node should be consistent with the actual voltages and currents of this node in the distribution network.

Step (b) Searching of questionable nodes

Calculate the voltages at next nodes and currents flowing into the next nodes from all normal nodes (with known voltages and currents) using normal operating condition model of the line sections. The node can be considered as a questionable node when two of the calculated voltages at this node are not consistent (with the absolute difference exceeding a certain user-defined threshold). In this case, the line section which leads to a different voltage compared to the results from other line sections (at least two other line sections) is considered as the line with fault. Then, the faulted line identification is paused. The node can be considered as a normal node when the calculated N-1 section at this node are approximately equal (where N is the number of line sections connecting to any node, at least 3). In this case, the (N-1) currents flowing into this node can also be calculated. Therefore, from KCLs of this node, the current flowing into the last line section connecting to this node can also be calculated (if necessary). This current will be utilized in the next iteration. Step (b) will be repeated until all nodes are checked.

For Figure 2, the fault occurs in line section L11. In the first iteration, node 10 will be considered as a normal node, since the voltages at node 10 calculated from M1, M2 and M3 are the same. In the second iteration, since the voltage at node 10 and the current flowing from node 10 to node 11 have been calculated in the last iteration (as this current can be calculated from the KCLs at node 10), the voltage at node 11 can also be calculated. After several iterations, one can find that the voltages at node 13 are not consistent: the voltage calculated through line section L11 (using voltages and currents from node 11) is not consistent with voltages calculated through the other two line sections L13 and L6. Therefore, the faulted line section is determined as L11.

B. Fault location algorithm

The overall line model in (5) can be generated with known faulted section. The state estimation algorithm is applied to solve the state vector x in (5), i.e., the fault location. Here the weighted least square method is utilized, that is,

$$\min J = \left(f(\boldsymbol{x}) - \boldsymbol{z}\right)^T \boldsymbol{W} \left(f(\boldsymbol{x}) - \boldsymbol{z}\right) \tag{6}$$

where $\boldsymbol{W} = diag\{1/\sigma_1^2 \;\; 1/\sigma_2^2 \;\cdots\}$ is the weight matrix and $\sigma_i \left(i = 1, 2, \cdots\right)$ is the standard deviation of the i^{th} measurement.

The estimated state vector $\hat{\boldsymbol{x}}$ is given by the following Newton's iterative method until convergence:

$$\boldsymbol{x}^{n+1} = \boldsymbol{x}^n - \left(\boldsymbol{H}^T \boldsymbol{W} \boldsymbol{H}\right)^{-1} \boldsymbol{H}^T \boldsymbol{W} \left(f(\boldsymbol{x}^n) - \boldsymbol{z}\right) \tag{7}$$

where the Jacobian matrix is $\boldsymbol{H} = \partial f(\boldsymbol{x}) / \partial \boldsymbol{x}\big|_{x=x^n}$.

IV. Simulation Results

The proposed fault location method is verified via the example active distribution network, as shown in Figure 1. Rated voltage and capacity of this system are 35kV and 10MVA respectively. Three phase sources S1, S2 and S3 are connected to the active distribution network, with source S1 as the main power grid and source S2 and source S3 as DGs. The rated frequency of this system is 50 Hz. The length of the lines L1~L14 are: 10, 9, 8, 11, 12, 10, 9, 8, 8, 10, 20, 10, 10 and 8 km respectively. The distribution system works with the unbalanced condition and the distribution lines are asymmetry. The voltage and current phasor measurements are installed at terminal M1~M9. The phasors are calculated according to IEEE C37.118 standard (the sampling rate of the raw data is 80 samples per cycle). The distribution lines are simulated using the Bergeron line model in PSCAD/EMTDC.

In order to verify the performance of the proposed fault location method, numerous fault events with different fault locations, fault types and fault impedances are simulated. Due to space limitations, four groups of events with different fault types are studied, including phase A to ground faults, phase B to C faults, phase B and phase C to ground faults and three-phase faults. Four groups of events with different fault impedances are studied, including 2 ohm, 5 ohm, 8 ohm and 20 ohm. The user-defined threshold for the faulted line identification is 0.4 kV. Detailed results of faulted line identification and fault location are shown as follows. The absolute error of the fault location is defined as,

$$\text{Abs error}(\%) = \left|\frac{\text{Estimated location-Actual location}}{\text{Length of the line L11}}\right| \times 100\% \tag{8}$$

A. Faulted line identification

Here a phase A to ground fault is taken as an example. A phase A to ground fault occurs at time 0.3s and 15 km away from the node 11 of the line L11 with 0.01ohm fault impedance. The detailed performance of faulted line identification is depicted in Figure 3. The line index 1-14 represents line L1 to line L14.

From Figure 3, the identification result varies during 0.3s to 0.333s and converged to line L11 at 0.333s. This result shows that the faulted line identification method is reliable after the transient period of 1.665 cycles. The varying identification result at the first 1.665 cycles is due to the transients of the system and inaccuracy of phasor representation of the system during transients. The results could be improved if advanced phasor calculation method (eg. with DC offset removal) is applied instead of IEEE C37.118 standard. However, this result is acceptable in practice especially for distribution networks. With the faulted line identification result, fault location can be obtained via the next step.

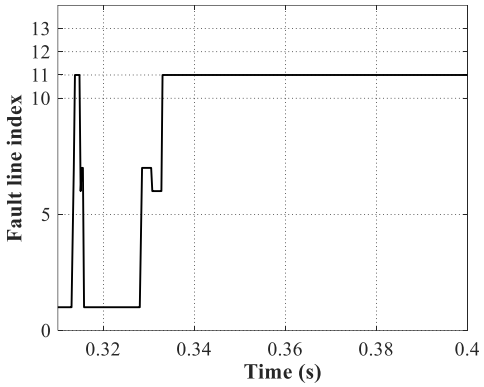

Figure 3. Faulted line identification result: Phase A to ground fault at line L11

B. Fault location

The detailed results of the proposed fault location method with different groups of fault events are demonstrated next. Note that the overall line model in (5) can be classified into the overall model without shunt admittance (denoted as method 1) and the overall model with shunt admittance (denoted as method 2).

(1) Performance with different fault types

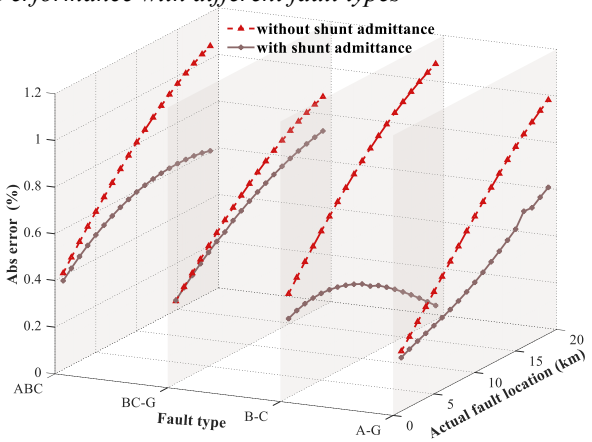

Figure 4. Fault location results of two methods with different fault types and 0.01ohm fault impedance

Table 2. Summary of the fault location results with different fault types and 0.01 ohm fault impedance

Fault type	Method index	Max absolute error(%)	Average absolute errors(%)
A-N	1	1.00	0.65
	2	0.63	0.41
B-C	1	1.10	0.82
	2	0.37	0.27
BC-N	1	0.90	0.67
	2	0.75	0.59
ABC	1	1.05	0.78
	2	0.62	0.56

To further validate the effectiveness of the proposed method, the events at different fault locations (every 1km, through the line) with different fault types (phase A to ground fault, phase B to phase C fault, phase B and phase C to ground fault and three-phase fault) and 0.01 ohm fault impedance are tested. The fault location results of two methods are depicted in Figure 4. The summary of the fault location results of two methods are shown in Table 2.

(2) Performance with different fault impedances

To further validate the effectiveness of the proposed method, the events at different fault locations (every 1km, through the line) with phase A to ground fault and different fault impedances (2 ohm, 5 ohm, 8 ohm, 20 ohm) are tested. The fault location results of two methods are depicted in Figure 5. The summary of the fault location results of two methods are shown in Table 3.

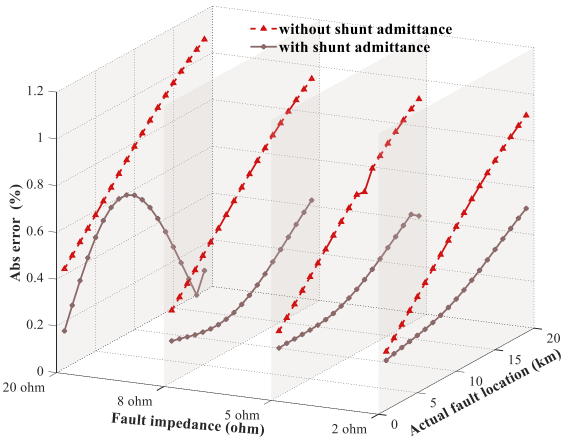

Figure 5. Fault location results of two methods with phase A to ground fault and different fault impedances

Table 3. Summary of the fault location results with phase A to ground fault and different fault impedances

Fault impedance (ohm)	Method index	Max absolute error(%)	Average absolute errors(%)
2	1	0.93	0.61
	2	0.53	0.34
5	1	0.94	0.62
	2	0.46	0.29
8	1	0.97	0.66
	2	0.45	0.23
20	1	1.08	0.77
	2	0.60	0.36

From above fault location results, it can be observed that the method without shunt admittance and the method with shunt admittance both perform relatively well and obtain accepted results with different fault types and fault impedances. Moreover, the method with shunt admittance presents more accurate fault location result compared to the method without shunt admittance.

V. Conclusion

A novel state estimation based fault location method for the active distribution networks is proposed in this paper. The three phase voltage and current phasor measurements at terminals of the network are assumed. The overall model of the active distribution network with fault is established by combining the distribution line model of each section. The three phase matrix representation of physical laws of the distribution line is utilized. This method can systematically consider the network configuration, the shunt admittance and the asymmetry of the distribution line. The fault location algorithm contains two steps: faulted line section identification and accurate fault location inside the specific faulted line section. The methods with and without shunt admittance are verified via the numerical experiments. The results demonstrate that both two methods perform relatively well and yield accepted results in active distribution systems with DGs, with different fault types, fault impedances, unbalanced distribution systems, and asymmetrical distribution lines. It is shown that the method considering shunt admittance can obtain more accurate fault location results.

References

[1] *IEEE Std C37. 114-2004*, IEEE Guide for Determining Fault Location on AC Transmission and Distribution Lines, 2005

[2] M. Kezunovic, "Smart Fault Location for Smart Grids," *IEEE Trans. Smart Grid*, vol. 2 no. 1, Mar. 2011, pp. 11 – 22.

[3] K. Srinivasan, A.S. Jacques, "A New Fault Location Algorithm for Radial Transmission Lines With Loads," *IEEE Trans. Power Del.*, vol. 4, no. 3, Jul. 1989, pp. 1676 – 1682.

[4] R.H. Salim, K.C.O. Salim, A.S. Bretas, "Further Improvements on Impedance-Based Fault Location for Power Distribution Systems," *IET Gener. Transm. Distrib.*, vol. 5, no. 4, Mar. 2011, pp. 467-478.

[5] M. Choi, S. Lee, D. Lee, and B. Jin, "A New Fault Location Algorithm Using Direct Circuit Analysis for Distribution Systems," *IEEE Trans. Power Del.*, vol. 19, no. 1, Jan. 2004, pp. 35 – 41.

[6] M. Choi, S. Lee, D. Lee, and X. Yang, "A Direct Three-Phase Circuit Analysis-Based Fault Location for Line-to-Line Fault," *IEEE Trans. Power Del.*, vol. 22, no. 4, Oct. 2007, pp. 2541 – 2547.

[7] A. Dwivedi and X. Yu, "Fault Location in Radial Distribution Lines Using Travelling Waves and Network Theory," in *Proc. IEEE International Symposium on Industrial Electronics*, Gdansk, 2011, pp. 1051-1056.

[8] D. W. P. Thomas, R. J. O. Carvalho and E. T. Pereira, "Fault Location in Distribution Systems Based on Traveling Waves," in *Proc. IEEE Bologna Power Tech Conference Proceedings*, Bologna, Italy, 2003, pp. 5.

[9] S. Shi, B. Zhu, A. Lei and X. Dong, "Fault Location for Radial Distribution Network via Topology and Reclosure-Generating Traveling Waves," *IEEE Trans. Smart Grid*, vol. 10, no. 6, Nov. 2019, pp. 6404 – 6413.

[10] J. Teng, W. Huang and S. Luan, "Automatic and Fast Faulted Line-Section Location Method for Distribution Systems Based on Fault Indicators," *IEEE Trans. Power Del.*, vol. 29, no. 4, Jul. 2014, pp. 1653 – 1662.

[11] A. N. Milioudis, G. T. Andreou and D. P. Labridis, "Detection and Location of High Impedance Faults in Multiconductor Overhead Distribution Lines Using Power Line Communication Devices," *IEEE Trans. Smart Grid*, vol. 6, no. 2, Mar. 2015, pp. 894 – 902.

[12] S. Lotfifard, M. Kezunovic and M. J. Mousavi, "Voltage Sag Data Utilization for Distribution Fault Location," *IEEE Trans. Power Del.*, vol. 26, no. 2, Apr. 2011, pp. 1239 – 1246.

[13] S. Lee, M. Choi, S. Kang, B. Jin, D. Lee, B. Ahn, N. Yoon, H. Kim and S. Wee, "An Intelligent and Efficient Fault Location and Diagnosis Scheme for Radial Distribution Systems," *IEEE Trans. Power Del.*, vol. 19, no. 2, Apr. 2004, pp. 524 – 532.

[14] J. M. Florez, V. B. Núñez, and G. C. Caicedo, "Fault Location in Power Distribution Systems Using a Learning Algorithm for Multivariable Data Analysis," *IEEE Trans. Power Del.*, vol. 22, no. 3, Jul. 2007, pp. 1715-1721.